Nonrelativistic trace anomaly and equation of state in dense fermionic matter

Hiroyuki Tajima [1], Kei Iida [2], and Haozhao Liang [1,3]

[1]*Department of Physics, Graduate School of Science, The University of Tokyo, Tokyo 113-0033, Japan*
[2]*Department of Mathematics and Physics, Kochi University, Kochi 780-8520, Japan*
[3]*RIKEN Interdisciplinary Theoretical and Mathematical Sciences Program, Wako 351-0198, Japan*

(Received 8 February 2024; accepted 23 April 2024; published 14 May 2024)

We investigate theoretically a nonrelativistic trace anomaly and its impact on the low-temperature equation of state in spatially one-dimensional three-component fermionic systems with a three-body interaction, which exhibit a nontrivial three-body crossover from a bound trimer gas to dense fermionic matter with increasing density. By applying the G-matrix approach to the three-body interaction, we obtain the analytical expression for the ground-state equation of state relevant to the high-density degenerate regime and thereby address how the three-body contact or, equivalently, the trace anomaly emerges. The analytical results are compared with the recent quantum Monte Carlo data. Our study of the trace anomaly and the sound speed could have some relevance to the physics of hadron-quark crossover in compact stars.

DOI: 10.1103/PhysRevC.109.055203

I. INTRODUCTION

The recent development of astrophysical observations enables us to address the fundamental question of how matter behaves at extremely high density. Indeed, masses and radii of neutron stars have been simultaneously deduced from gravitational waves observed from a binary neutron-star merger [1]. By incorporating such information and the presence of a heavy neutron star [2] into a Bayesian analysis, the equation of state of neutron-star matter has been determined, such that the speed of sound is marginally peaked at several times of the normal nuclear density $\rho_0 = 0.16\ \mathrm{fm}^{-3}$ [3]. In a manner that is consistent with this equation of state, nowadays we are in a position to theoretically construct the equation of state of matter at densities significantly higher than ρ_0.

In such an extremely dense environment, hadrons, which consist basically of three quarks, overlap with each other and can no longer be regarded as point-like particles. Eventually, neutron-star matter is expected to be governed by the quark degrees of freedom in the form of color superconducting quark matter [4]. It is nevertheless difficult to figure out how nuclear matter, which is relatively well known, changes into such quark matter as density increases. The above-mentioned empirical equation of state of neutron-star matter invokes the so-called hadron-quark crossover scenario [5–7], where nuclear matter, if compressed, would undergo a crossover toward quark matter rather than a phase transition [8,9]. While its microscopic mechanism is still elusive in the presence of the sign problem inherent in lattice simulations of finite-density quantum chromodynamics (QCD), a recent lattice simulation of finite-density two-color QCD [10,11], which is free of the sign problem, indicates a peak in the speed of sound in the density region, where the diquark condensate gradually changes in a similar way to the Bose-Einstein condensation (BEC)-to-Bardeen-Cooper-Schrieffer (BCS) crossover [12–19] realized in ultracold Fermi atomic gases [20–22].

In this sense, an alternative promising route to address the microscopic mechanism of the hadron-quark crossover could be via an analog quantum simulation based on ultracold atomic physics [23–25]. Thanks to the tunable interactions, adjustable internal degrees of freedom, and reachable quantum degeneracy through Feshbach resonances, hyperfine states, and state-of-the-art cooling techniques, respectively, ultracold atoms offer an ideal platform to investigate quantum many-body physics [26]. Indeed, for a nonrelativistic one-dimensional (1D) three-component Fermi atom mixture with a three-body interaction between different components, a crossover from a gas of tightly bound trimers to a gas of single atoms with increasing density has been pointed out [27]; the thermal equation of state and the minimum of the compressibility (corresponding to the sound velocity peak) in the crossover regime have been reported from a quantum Monte Carlo (QMC) simulation based on the worldline formulation, which is free of the sign problem [28]. Such a system can be regarded as a good testing ground for many-body theories involving three-body forces, which play a crucial role in low-energy nuclear physics [29,30]. The topological aspects of the three-body interaction have also been investigated theoretically [31–33].

Furthermore, this 1D system exhibits a trace anomaly [34] due to the broken scale invariance [27,35]. The same kind of trace anomaly is known to appear in spatially three-dimensional (3D) dense QCD, which has been recently

discussed in connection with the sound velocity peak [36]. Note that, in both systems, the trace anomaly corresponds to the deviation of the equation of state from the scale-invariant behavior in the high-density limit. In the nonrelativistic system, which will be studied here, the trace anomaly can be expressed in terms of the three-body contact [27,35], which is a three-body generalization of Tan's two-body contact [37–39] and characterizes the probability of finding three particles close to each other [40,41]. The numerical values of the three-body contact in the crossover regime have also been obtained from the above-mentioned QMC simulation [28].

It is useful to consider various spatial dimensions and multibody interactions in the nonrelativistic Fermi system of interest here. The trace anomaly has been experimentally measured in spatially two-dimensional (2D) two-component Fermi atomic gases with two-body interaction [42,43], while it has been theoretically shown that in the high-temperature limit, there is an exact mapping of the two-body anomalous interaction in the 2D model onto the three-body anomalous interaction in the 1D model [44]. Incidentally, both models are asymptotically free: The interactions become asymptotically weaker with increasing density. Intuitively, this can be understood from the comparison of two energy scales, namely, the Fermi energy $E_{\rm F}$ and the multibody binding energy $E_{\rm b}$; the weak-coupling limit is realized when $E_{\rm F}/E_{\rm b} \to \infty$. This property is in contrast with the conventional 3D model where the energy ratio is characterized by the Fermi momentum $k_{\rm F}$ and the two-body scattering length a in such a way that the high-density limit corresponds to the unitarity (i.e., $k_{\rm F}|a| \to \infty$) [19].

In considering the crossover mechanism of nonrelativistic three-component Fermi mixtures, it is interesting to focus on the analogy with the BEC-BCS crossover in two-component Fermi atomic gases, where tightly bound diatomic molecules are changed into overlapped bound Cooper pairs. Indeed, in three-component Fermi atomic gases, one can expect a similar crossover where tightly bound triatomic molecules are changed into overlapped bound trimers called Cooper triples [45,46]. Such a triple state that persists even in the presence of a Fermi sea is a natural extension of the Cooper pairing state and partially consistent with a phenomenological picture of quarkyonic matter that is favorable for explaining the sound velocity peak in neutron-star matter [47]. The crossover from baryons to color-singlet Cooper triples has also been discussed theoretically in a semirelativistic quark model with a phenomenological three-body attraction that is responsible for color confinement [48]. However, it remains to be investigated how the ground-state equation of state is associated with the three-body correlations and the trace anomaly even in the high-density regime of neutron-star matter.

In this work, we theoretically investigate the ground-state equation of state for nonrelativistic 1D three-component fermionic matter, which is connected to the trace anomaly just like dense QCD, by using the Brueckner G-matrix approach, which is known to successfully describe the ground-state equation of state for asymptotically free 2D Fermi atomic gases [49–51]. Remarkably, this approach gives an analytical expression for the equation of state, which in turn well reproduces the equation of state obtained by a QMC simulation [52] and experiments [53,54] throughout the 2D BCS-BEC crossover. Moreover, the G-matrix result for the ground-state energy of a Fermi polaron, namely, an impurity quasiparticle immersed in a Fermi sea, shows an excellent agreement with the exact result in 1D [55] and experimental results in 2D [56]. We focus on the low-temperature and high-density regime where the QMC simulation is numerically demanding even in this nonrelativistic 1D system regardless of the fact that the high-density regime corresponds to the weakly coupled regime due to the asymptotic freedom. In particular, we derive an analytical expression for the equation of state and the three-body contact in this system and elucidate the impact of the trace anomaly on the ground-state equation of state in the presence of strong three-body correlations.

This paper is organized as follows: In Sec. II, we present a formalism for describing nonrelativistic 1D three-component fermions involving three-body attractive interaction. In Sec. III, we discuss the three-body contact and the ground-state equation of state in the high-density regime ($\mu > 0$). We summarize this paper in Sec. IV. Throughout the paper, we take $\hbar = k_{\rm B} = 1$. and the system size is set to be unity.

II. FORMALISM

We consider nonrelativistic 1D three-component fermions by starting from the following Hamiltonian [27,44],

$$H = \sum_{a={\rm r,g,b}} \sum_{j_a}^{N_a} \frac{1}{2m}\left(-\frac{\partial^2}{\partial x_{j_a}^2}\right) + \sum_{j_{\rm r},j_{\rm g},j_{\rm b}} g_3 \delta\left(x_{j_{\rm r}} - x_{j_{\rm g}}\right)\delta\left(x_{j_{\rm g}} - x_{j_{\rm b}}\right), \tag{1}$$

where the first term describes the kinetic energy of a fermion with mass m and color index $a = {\rm r, g, b}$, and g_3 is the coupling constant of contact-type three-body interaction among different colors. N_a is the number of fermions of color a. One can see that even in the presence of nonzero g_3, the Schrödinger equation $(i\frac{\partial}{\partial t} - H)\Psi = 0$ is invariant under the scale transformation of $x_j \to \lambda x_j$ and $t \to \lambda^2 t$, where Ψ is the many-fermion wave function [57]. The second quantized form of H reads

$$H = \int \frac{dp}{2\pi} \sum_{a={\rm r,g,b}} \epsilon_p \psi_{p,a}^\dagger \psi_{p,a} + g_3 \int \frac{dKdkdqdk'dq'}{(2\pi)^5} F^\dagger(k,q,K)F(k',q',K), \tag{2}$$

where $\epsilon_p = p^2/(2m)$ is the kinetic energy of a fermion, and $\psi_{p,a}$ is the fermion operator. The three-body interaction can be expressed in terms of the three-fermion operator,

$$F(k,q,K) = \frac{1}{6}\sum_{a_1,a_2,a_3} \varepsilon_{a_1a_2a_3} \times \psi_{\frac{K}{3}-q,a_1}\psi_{\frac{K}{3}-k+\frac{q}{2},a_2}\psi_{\frac{K}{3}+k+\frac{q}{2},a_3}, \tag{3}$$

where $\varepsilon_{a_1a_2a_3}$ is the completely antisymmetric tensor.

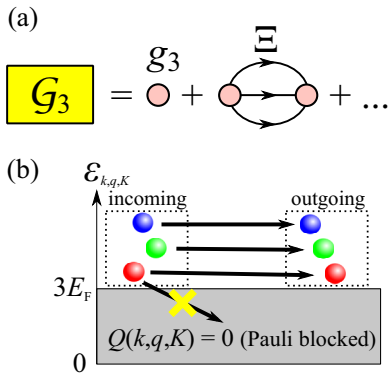

FIG. 1. (a) Feynman diagrams for the three-body G matrix $\mathcal{G}_3(K,\omega)$. The circle represents the three-body coupling g_3. Three solid lines correspond to the three-body propagator $\Xi(K,\omega)$. (b) Schematics of the Tamm-Dancoff approximation for virtual three-particle states in Ξ. The Pauli-blocking factor $Q(k,q,K)$ becomes zero when the three-particle kinetic energy $\mathcal{E}_{k,q,K}$ is less than $3E_F$, where E_F is the Fermi energy.

The three-body coupling constant g_3 induces a three-body bound state even for infinitesimally small g_3 in 1D, which breaks the classical scale invariance at quantum level. Because of nonperturbative properties of the three-body coupling, we need to sum up an infinite series of the three-body ladder diagrams shown in Fig. 1(a) even in the weak-coupling (or high-density) regime. The three-body G matrix is given by

$$\mathcal{G}_3(K,\omega) = \left[\frac{1}{g_3} - \Xi(K,\omega)\right]^{-1}, \tag{4}$$

where

$$\Xi(K,\omega) = \int \frac{dkdq}{(2\pi)^2}\frac{Q(k,q,K)}{\omega - \mathcal{E}_{k,q,K}} \tag{5}$$

is the three-body propagator with the Pauli-blocking factor $Q(k,q,K)$, and $\mathcal{E}_{k,q,K}$ is the kinetic energy of three particles given by

$$\mathcal{E}_{k,q,K} = \frac{\left(\frac{q}{2}+\frac{K}{3}+k\right)^2}{2m} + \frac{\left(\frac{K}{3}-q\right)^2}{2m} + \frac{\left(\frac{q}{2}+\frac{K}{3}-k\right)^2}{2m}. \tag{6}$$

The three-body coupling can be characterized by the three-body binding energy E_b in vacuum obtained from the pole of the three-body T matrix [46]. Namely, we take $Q(k,q,K) = 1$ in Eq. (5) and obtain

$$\frac{1}{g_3} = -\int \frac{dkdq}{(2\pi)^2}\frac{1}{E_b + \mathcal{E}_{k,q,0}} = -\frac{m}{2\sqrt{3}\pi}\ln\left(\frac{mE_b+\Lambda^2}{mE_b}\right), \tag{7}$$

where Λ is the momentum cutoff. In this regard, one can find that a usual Hartree-like lowest-order interaction energy $g_3\rho_r\rho_b\rho_g$, where ρ_a is the number density of color a, vanishes in the limit of $\Lambda\to\infty$, indicating that an appropriate regularization of Λ is needed even in the high-density limit. We note that the appearance of E_b, which is a dimensional quantity, from the scale-invariant coupling $g_3 \sim m^{-1}$ is the consequence of the trace anomaly [27]. Its impact on the ground-state equation of state will be addressed below.

Hereafter, we focus on the color-symmetric case with $\rho_r = \rho_b = \rho_g \equiv \rho/3$, where ρ is the total number density. Following the idea of the Brueckner Hartree-Fock theory in the presence of a bound state [49–51], we evaluate the internal energy E as the Hartree-Fock-like expectation value $E = \langle H\rangle$ by replacing g_3 with the in-medium effective interaction $\mathcal{G}_3(K = 0, \omega = -E_b)$, that is,

$$E = \tfrac{1}{3}\rho E_F + \tfrac{1}{27}\mathcal{G}_3(0,-E_b)\rho^3. \tag{8}$$

This approximation leads to an analytical expression for the equation of state, which works unexpectedly well in two-dimensional two-component Fermi atomic gases with attractive interaction throughout the BCS-BEC crossover [50,51] (see also the Appendix).

As schematically shown in Fig. 1(b), we evaluate $\Xi(0,-E_b)$ in $\mathcal{G}_3(0,-E_b)$ within the Tamm-Dancoff approximation where hole-like excitations are suppressed at $T = 0$ [58]. This treatment is similar to the generalized Cooper problem for three-body states without any hole excitations [45,59–62]. As in the case of 2D two-component Fermi gases in which the states with zero center-of-mass momentum can be regarded as the relevant contribution, the states with $K = 0$, which correspond to squeezed Cooper triples, can be relevant in 1D three-component Fermi gases [45,46]. Because of the internal degrees of freedom associated with constituent fermions in three-body cluster states, the three-body correlations at $K = 0$ involve an ultraviolet divergence with respect to the integration of relative momenta. Although we do not consider the condensation in the present 1D system, the low-momentum correlations play a crucial role at low temperature and high density; indeed, such an approximation shows a good agreement with experiments [53,54,56] as well as QMC simulations [40,63] as shown in Refs. [49–51]. On the other hand, our approach cannot reproduce the low-density limit where a gas of tightly bound trimers is realized because we do not consider three-body correlations with $K \neq 0$. In this regard, we focus on the high-density regime where the contribution with $K = 0$ can be expected to be dominant. By introducing $\bar{q} = \frac{\sqrt{3}}{2}q$ and $r = (k^2+\bar{q}^2)^{1/2}$, we obtain

$$\Xi(0,-E_b) = -\frac{m}{2\sqrt{3}\pi^2}\int_0^\Lambda 2\pi r dr \frac{Q\left(k,\frac{2}{\sqrt{3}}\bar{q},0\right)}{mE_b + r^2}. \tag{9}$$

Note here that $r^2 = m\mathcal{E}_{k,q,0} \geqslant 3mE_F$. Then, we find $Q(k,\frac{2}{\sqrt{3}}\bar{q},0) \equiv Q(r) = \theta(r - \sqrt{3/2}k_F)$ with the Fermi momentum $k_F = \pi\rho/3$, leading to

$$\Xi(0,-E_b) = -\frac{m}{2\sqrt{3}\pi}\ln\left(\frac{mE_b+\Lambda^2}{mE_b+\frac{3}{2}k_F^2}\right). \tag{10}$$

Accordingly, we obtain

$$\mathcal{G}_3(0,-E_b) = -\frac{2\sqrt{3}\pi}{m}\left[\ln\left(\frac{mE_b+\frac{3}{2}k_F^2}{mE_b}\right)\right]^{-1}. \tag{11}$$

One can see that $\mathcal{G}_3(0,-E_b)$ in Eq. (11) does not depend on Λ in contrast with g_3 in Eq. (7).

Eventually, the internal energy within the present approach reads

$$E = \frac{1}{3}\rho E_{\rm F} - \frac{4\sqrt{3}}{3\pi}\rho E_{\rm F}\frac{1}{\ln\left(1+\frac{3E_{\rm F}}{E_{\rm b}}\right)}. \tag{12}$$

In particular, it is worth mentioning that in the high-density limit ($E_{\rm F} \gg E_{\rm b}$) one can obtain

$$E \simeq \frac{1}{3}\rho E_{\rm F} - \frac{4\sqrt{3}}{3\pi}\rho E_{\rm F}/\ln\left(\frac{3E_{\rm F}}{E_{\rm b}}\right). \tag{13}$$

While the G-matrix approach can be justified in the high-density regime due to the asymptotic freedom, the logarithmic correction in Eq. (13) is the consequence of nonperturbative nature of the three-body coupling captured by the infinite ladder resummation in Fig. 1(a).

Incidentally, while $Q(r) \equiv \theta(\mathcal{E}_{k,q,0} - 3E_{\rm F})$ certainly suppresses virtual states that satisfy $\mathcal{E}_{k,q,0} < 3E_{\rm F}$, our approach may underestimate the Pauli-blocking effect since virtual states involving one or two particles far above the Fermi sea and the rest inside the Fermi sea cannot be suppressed. Even so, it is still useful to find such an analytical formula for the equation of state by analogy with the 2D BEC-BCS crossover discussed in the Appendix and further improvements will be left as future work.

Some other thermodynamic quantities can be obtained via the thermodynamic identities. The chemical potential $\mu = \partial E/\partial\rho$ is given by

$$\frac{\mu}{E_{\rm F}} = 1 - \frac{4\sqrt{3}}{\pi}\frac{1}{\ln\left(1+\frac{3E_{\rm F}}{E_{\rm b}}\right)} + \frac{8\sqrt{3}}{3\pi}\frac{3E_{\rm F}/E_{\rm b}}{\left(1+\frac{3E_{\rm F}}{E_{\rm b}}\right)\left[\ln\left(1+\frac{3E_{\rm F}}{E_{\rm b}}\right)\right]^2}. \tag{14}$$

The pressure $P = \mu\rho - E$ reads

$$P = \frac{2}{3}\rho E_{\rm F} - \frac{8\sqrt{3}}{3\pi}\rho E_{\rm F}\frac{1}{\ln\left(1+\frac{3E_{\rm F}}{E_{\rm b}}\right)} + \frac{8\sqrt{3}}{3\pi}\rho E_{\rm F}\frac{3E_{\rm F}/E_{\rm b}}{\left(1+\frac{3E_{\rm F}}{E_{\rm b}}\right)\left[\ln\left(1+\frac{3E_{\rm F}}{E_{\rm b}}\right)\right]^2}. \tag{15}$$

In the high-density limit where $E_{\rm b}$ is negligible compared with $E_{\rm F}$, one can find the scale-invariant result $P = 2E$ [27].

However, at lower densities, such a relation is gradually broken due to the trace anomaly, which is equivalent to the three-body contact $C_3 = P - 2E$ [35]. To be self-contained, we show how the trace anomaly appears as the three-body contact in the equation of state of the present system by following the argument in Ref. [27]. At $T = 0$, E depends on ρ alone in the scale-invariant system; its form can be specified by the dimensional analysis as $E = \xi\rho E_{\rm F} \equiv \xi\pi^2\rho^3/18m$ with some constant ξ. In such a case, one can obtain $P = 2E$ by using the thermodynamic identities as $P = \mu\rho - E \equiv \rho(\partial E/\partial\rho) - E$. If the scale invariance is broken due to the trace anomaly accompanied by the emergence of the quantum-mechanical scale $E_{\rm b}$, it should be generalized as

$$E = \xi(e_{\rm b})\rho E_{\rm F}, \tag{16}$$

where $\xi(e_{\rm b})$ becomes a function of the dimensionless parameter $e_{\rm b} = E_{\rm b}/E_{\rm F}$. Then, one finds

$$P = 2E - 2\rho E_{\rm b}\frac{\partial\xi(e_{\rm b})}{\partial e_{\rm b}}. \tag{17}$$

The second term of Eq. (17) is nothing more than the correction of the trace anomaly on the equation of state. Since $\partial\xi(e_{\rm b})/\partial e_{\rm b}$ can be regarded as the change of E with respect to $E_{\rm b}$ for fixed $E_{\rm F}$ (or ρ), we obtain

$$\frac{\partial\xi(e_{\rm b})}{\partial e_{\rm b}} = \frac{1}{\rho}\frac{\partial E}{\partial E_{\rm b}} \equiv \frac{1}{\rho}\frac{\partial\langle V\rangle}{\partial g_3}\frac{\partial g_3}{\partial E_{\rm b}}, \tag{18}$$

where $\langle V\rangle \propto g_3$ is the expectation value of the interaction term in H. Taking the derivative of Eq. (10) with respect to $E_{\rm b}$, we obtain

$$E_{\rm b}\frac{\partial g_3}{\partial E_{\rm b}} = -\frac{m}{2\sqrt{3}\pi}g_3^2. \tag{19}$$

Combining Eqs. (17)–(19), we can find $P = 2E + C_3$ with the three-body contact [27]

$$C_3 = \frac{m}{\sqrt{3}\pi}g_3\langle V\rangle, \tag{20}$$

where we have used $g_3\partial\langle V\rangle/\partial g_3 = \langle V\rangle$ at $g_3 \to 0$ ($\Lambda \to \infty$).

In the present approximation, we can obtain $\xi(e_{\rm b})$ from Eq. (12) as

$$\xi(e_{\rm b}) = \frac{1}{3} - \frac{4\sqrt{3}}{3\pi}\frac{1}{\ln(1+3/e_{\rm b})}. \tag{21}$$

Note that $C_3 = -2\rho E_{\rm b}\partial\xi(e_{\rm b})/\partial e_{\rm b}$. We thus obtain

$$C_3 = \frac{8\sqrt{3}}{3\pi}\rho E_{\rm F}\frac{3E_{\rm F}/E_{\rm b}}{\left(1+\frac{3E_{\rm F}}{E_{\rm b}}\right)\left[\ln\left(1+\frac{3E_{\rm F}}{E_{\rm b}}\right)\right]^2}. \tag{22}$$

One can easily find that C_3 is positive definite as in the case of conventional Tan's contact [37–39].

Moreover, one can obtain the squared sound velocity $c_s^2 = \frac{1}{m}(\partial P/\partial\rho)$ as

$$\frac{c_s^2}{v_{\rm F}^2} = 1 - \frac{4\sqrt{3}}{\pi}\frac{1}{\ln\left(1+\frac{3E_{\rm F}}{E_{\rm b}}\right)} + \frac{28\sqrt{3}}{\pi}\frac{E_{\rm F}}{E_{\rm b}}\frac{1}{\left(1+\frac{3E_{\rm F}}{E_{\rm b}}\right)\left[\ln\left(1+\frac{3E_{\rm F}}{E_{\rm b}}\right)\right]^2} - \frac{24\sqrt{3}}{\pi}\frac{E_{\rm F}^2}{E_{\rm b}^2}\frac{2+\ln\left(1+\frac{3E_{\rm F}}{E_{\rm b}}\right)}{\left(1+\frac{3E_{\rm F}}{E_{\rm b}}\right)^2\left[\ln\left(1+\frac{3E_{\rm F}}{E_{\rm b}}\right)\right]^3}, \tag{23}$$

where $v_{\rm F} = k_{\rm F}/m$ is the Fermi velocity and corresponds to the high-density conformal limit in this system. We note that at $T = 0$, c_s^2 is related to the compressibility $\kappa = \frac{1}{\rho}(\partial\rho/\partial P)$. By introducing the noninteracting compressibility $\kappa_0 = \rho/v_{\rm F}^2$, we find $\kappa/\kappa_0 = v_{\rm F}^2/c_s^2$.

III. RESULTS

First, we discuss the three-body contact C_3, which arises from the trace anomaly. In particular, we focus on the regime with $\mu > 0$ where the Fermi degeneracy of constituent

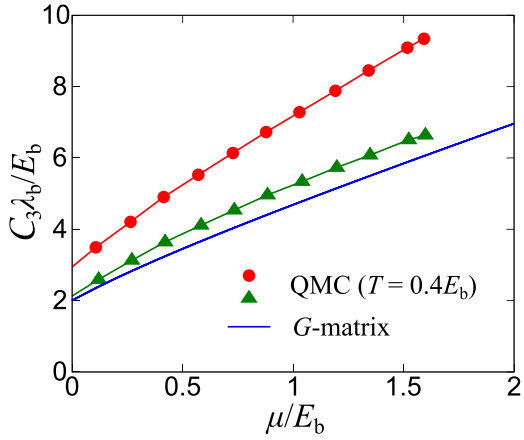

FIG. 2. Three-body contact C_3 as a function of μ/E_b at $T = 0$, where $\lambda_b = \sqrt{2\pi/mE_b}$ is the length scale associated with the three-body binding energy E_b. For comparison, we also show the QMC results at $T = 0.4E_b$ in Ref. [28], where the circles and triangles are evaluated by two different ways. These two results are different due possibly to lattice artifacts.

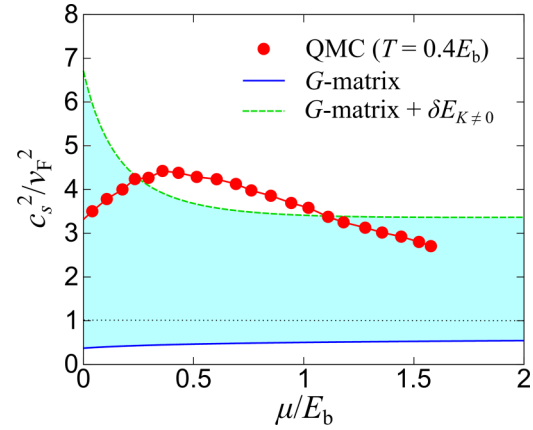

FIG. 4. Squared sound velocity c_s^2/v_F^2 as a function of μ/E_b, where v_F is the Fermi velocity corresponding to the conformal high-density limit. The solid and dashed curves represent the G-matrix results with and without the degenerate trimer contribution $\delta c^2_{K\neq 0}$, respectively. The circles show the QMC results obtained from $c_s^2/v_F^2 = \kappa_0/\kappa$ at $T = 0.4E_b$. The horizontal dotted line corresponds to the high-density limit ($c_s^2/v_F^2 = 1$).

fermions is important. Figure 2 shows C_3 as a function of μ/E_b at $T = 0$. One can see that C_3 increases with μ, indicating the importance of the low-energy three-body correlations which are reminiscent of squeezed Cooper triples [46]. We note that this increment is also associated with the increase of ρ as C_3 is normalized by the density-independent scales $\lambda_b = \sqrt{2\pi/mE_b}$ and E_b in Fig. 2. If we use the density-dependent scale (e.g., $C_3/\rho E_F$), such a quantity vanishes and hence the scale-invariant result $C_3/\rho E_F = (P - 2E)/\rho E_F \to 0$ is recovered in the high-density limit. Even within our simplified approach, our result is close to the QMC results performed at finite temperature ($T = 0.4E_b$) in Ref. [28]. In the present G-matrix approach where C_3 is a little bit underestimated, we do not consider the three-body correlations with nonzero K and the trimer-trimer interaction [64], which may be the origin of such underestimation of C_3.

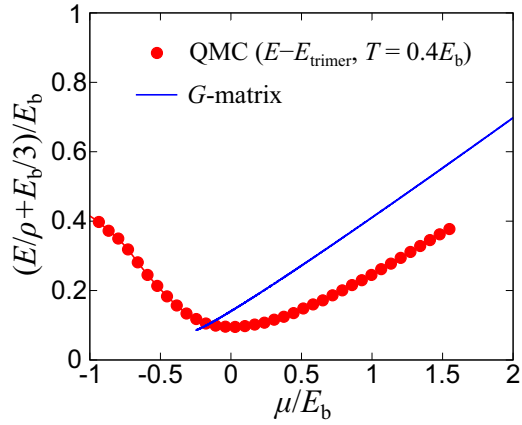

FIG. 3. Internal energy $(E/\rho + E_b/3)/E_b$ as a function μ/E_b. For comparison, the QMC result at $T = 0.4E_b$ in Ref. [28] is shown, where the plot has the trimer contribution E_{trimer} subtracted out.

Figure 3 shows the internal energy per particle $E/\rho + E_b/3$. In Ref. [28], the QMC results for the internal energy density E that has the trimer contribution $E_{trimer} = E_{TFG} - \rho E_b/3$ subtracted out were reported, where E_{TFG} is the internal energy density of a noninteracting trimer Fermi gas. Since E_{TFG} is not considered in our calculation, we compare the G-matrix result for $E/\rho + E_b/3$ with $(E - E_{trimer})/\rho$ in the QMC simulation. At $\mu > 0$, our result is qualitatively consistent with the QMC result as both results show linear increase with μ/E_b. This enhancement is also related to the increase of ρ. The quantity shown in Fig. 3 indicates the degree to which the system differs from a noninteracting trimer Fermi gas. In this sense, the result for C_3 obtained by the G-matrix approach may be regarded as the three-body correlations that cannot be described by the point-like trimer formation. On the other hand, the trimer-trimer repulsive interaction [64] is not considered in our calculation. This repulsion would act to increase E and thus lead to further discrepancy between the QMC simulation and the G-matrix approach.

Finally, we examine the squared sound velocity c_s^2/v_F^2 as shown in Fig. 4. For comparison, we also show the QMC result obtained from the dimensionless compressibility κ/κ_0 at $T = 0.4E_b$. Although the QMC result, which is above unity, involves the finite-temperature effect, the G-matrix result for c_s^2/v_F^2 is well below unity. To understand this discrepancy, we phenomenologically introduce the three-body correlations with nonzero center-of-mass momenta ($K \neq 0$) as $E \to E + \delta E_{K\neq 0}$ where

$$\delta E_{K\neq 0} = \int \frac{dK}{2\pi}\frac{K^2}{6m}\theta(K_T - K) = \frac{K_T^3}{18\pi m}. \tag{24}$$

In Eq. (24), $K_T = \sqrt{6m(3E_F + E_b)}$ is the effective trimer Fermi momentum. Then, using the thermodynamic identities, we find the associated correction to the squared sound velocity

$c_s^2 \to c_s^2 + \delta c_{s,K\neq 0}^2$, where

$$\delta c_{s,K\neq 0}^2 = \frac{k_{\rm F} K_{\rm T}}{2m^2} + \frac{9k_{\rm F}^3}{2m^2 K_{\rm T}}. \tag{25}$$

The dashed curve in Fig. 4 shows the result for $c_s^2/v_{\rm F}^2$ including the phenomenological three-body correlations with $K \neq 0$. Indeed, it is close to the QMC result. This indicates the importance of the Pauli pressure of in-medium trimers in addition to the trace anomaly in the high-density regime. On the other hand, $\delta c_{s,K\neq 0}^2$ does not vanish even in the high-density limit ($E_{\rm F} \gg E_{\rm b}$), whereas $c_s^2/v_{\rm F}^2$ should approach unity in the high-density limit. In this sense, the phenomenological expression for $\delta c_{s,K\neq 0}^2$ based on point-like trimer states overestimates the excess of c_s^2, implying that the nonlocal Cooper-triple-like correlations with $K \neq 0$ should be taken into account [46]. The trimer-trimer interaction would also play an important role in changing c_s^2, in addition to C_3 and E. Although the G-matrix result is known to follow $c_s^2/v_{\rm F}^2 \simeq 1 - 4\sqrt{3}/[\pi \ln(3E_{\rm F}/E_{\rm b})]$, which is consistent with the equation of state in the BCS-BEC crossover [50,51], therefore, a more detailed investigation of the high-density asymptotic behavior of c_s^2 is left for an important future work.

IV. SUMMARY

To summarize, we have investigated the trace anomaly and its impact on the ground-state equation of state for nonrelativistic 1D three-component fermions. By extending the G-matrix approach developed for the system with two-body interaction to the system with three-body interaction, we have obtained the analytical expression for the ground-state equation of state in the presence of three-body correlations that cannot be described by the formation of point-like trimers. The three-body contact, which results from the nonrelativistic trace anomaly, is found to increase with the chemical potential. Our results are qualitatively consistent with the recent QMC results at positive chemical potentials even within the simplified approximations adopted here. We expect that the Cooper-triple-like three-body correlations appear in the present system.

As for future perspectives, it is important to consider the three-body correlations with nonzero center-of-mass momenta as well as trimer-trimer interactions for further understanding of the three-body crossover equation of state. Finite-temperature effects should also be addressed for more quantitative comparison with the QMC calculation. Moreover, it would be interesting to apply the present approach to hadron-quark crossover by considering a system of constituent quarks interacting via a three-body color-confining force.

ACKNOWLEDGMENTS

The authors thank the members of the Low-Energy Nuclear Theory group at The University of Tokyo for useful discussion on these and related subjects and J. E. Drut for providing information on Ref. [28]. Also, H.T. is grateful to N. Yamamoto for useful discussion at the Workshop "Thermal Quantum Field Theory" held in KEK. This research was supported in part by Grants-in-Aid for Scientific Research provided by JSPS through Grants No. JP18H05406, No. JP22H01158, No. JP22K13981, No. JP23H01167, and No. JP23K25864.

APPENDIX: TRANSDIMENSIONAL SIMILARITY THROUGH THE NONRELATIVISTIC TRACE ANOMALY

Equation (12) for a 1D three-component Fermi gas with the zero-range three-body interaction shares a similarity with the corresponding internal energy $E_{\rm 2D}$ of a 2D two-component Fermi gas with zero-range two-body interaction as discussed in terms of few-body analyses and the virial expansion [27,44]. Indeed, the same approximation to the internal energy is applicable, leading to [50,51]

$$E_{\rm 2D} = \frac{1}{2}\rho E_{\rm F,2D} - \rho E_{\rm F,2D} \frac{1}{\ln\left(1 + \frac{2E_{\rm F,2D}}{E_{\rm b,2D}}\right)}, \tag{A1}$$

where $E_{\rm F,2D} = \pi\rho/m$ and $E_{\rm b,2D}$ are the Fermi energy and the two-body binding energy in a 2D two-component Fermi gas. An important advantage of Eq. (A1) is that it can reproduce the exact expressions in both weak BCS and strong BEC limits, which are given by $\rho E_{\rm F,2D}/2 - \rho E_{\rm F,2D}/\ln(2E_{\rm F,2D}/E_{\rm b,2D})$ at $E_{\rm b,2D}/E_{\rm F,2D} \to 0$ and $-\rho E_{\rm b,2D}/2$ at $E_{\rm b,2D}/E_{\rm F,2D} \to \infty$, respectively [50,51]. In this regard, Eq. (A1) qualitatively captures the BCS-BEC-crossover physics by interpolating the two opposite limits. In the present 1D case, Eq. (12) can also give the weak-coupling (high-density) limit given by Eq. (13), as in the case of 2D Fermi gases with two-body interaction [50,65]. Note, however, that Eq. (12) leads to $E \to -\frac{4\sqrt{3}}{27\pi}\rho E_{\rm b}$ at $E_{\rm b}/E_{\rm F} \to \infty$. While it is similar to the sum of the binding energy $-\rho E_{\rm b}/3$ for bound states of density $\rho/3$, the factor is different by $4\sqrt{3}/9\pi$. Since $-\rho E_{\rm b}/3$ is at odds with the Fermi degeneracy of a trimer gas, the smaller binding does not immediately indicate the breakdown of the present approach. Anyway, since Eq. (12) lacks the contribution of excited trimers with $K \neq 0$ which should be important in the low-density (strong-coupling) regime, we mainly discuss the high-density (weak-coupling) regime in the main text.

[1] B. P. Abbott *et al.* (LIGO Scientific Collaboration and Virgo Collaboration), Phys. Rev. Lett. **119**, 161101 (2017).
[2] P. B. Demorest, T. Pennucci, S. M. Ransom, M. S. E. Roberts, and J. W. T. Hessels, Nature (London) **467**, 1081 (2010).
[3] B. P. Abbott *et al.* (The LIGO Scientific Collaboration and Virgo Collaboration), Phys. Rev. Lett. **121**, 161101 (2018).
[4] M. G. Alford, A. Schmitt, K. Rajagopal, and T. Schäfer, Rev. Mod. Phys. **80**, 1455 (2008).

[5] T. Schäfer and F. Wilczek, Phys. Rev. Lett. **82**, 3956 (1999).
[6] G. Baym, T. Hatsuda, T. Kojo, P. D. Powell, Y. Song, and T. Takatsuka, Rep. Prog. Phys. **81**, 056902 (2018).
[7] T. Kojo, AAPPS Bull. (Online) **31**, 11 (2021).
[8] Y.-J. Huang, L. Baiotti, T. Kojo, K. Takami, H. Sotani, H. Togashi, T. Hatsuda, S. Nagataki, and Y.-Z. Fan, Phys. Rev. Lett. **129**, 181101 (2022).
[9] A. Kedia, H. I. Kim, I.-S. Suh, and G. J. Mathews, Phys. Rev. D **106**, 103027 (2022).
[10] K. Iida, E. Itou, and T.-G. Lee, J. High Energy Phys. (online) 01 (2020) 181.
[11] K. Iida and E. Itou, Prog. Theor. Exp. Phys. **2022**, 111B01 (2022).
[12] D. M. Eagles, Phys. Rev. **186**, 456 (1969).
[13] P. Nozières and S. Schmitt-Rink, J. Low Temp. Phys. **59**, 195 (1985).
[14] A. J. Leggett, in *Modern Trends in the Theory of Condensed Matter: Proceedings of the XVI Karpacz Winter School of Theoretical Physics, February 19–March 3, 1979 Karpacz, Poland*, edited by A. Pękalski and J. A. Przystawa, Lecture Notes in Physics, Vol. 115 (Springer, Karpacz, Polarnd, 2008), pp. 13–27.
[15] Q. Chen, J. Stajic, S. Tan, and K. Levin, Phys. Rep. **412**, 1 (2005).
[16] W. Zwerger, *The BCS-BEC Crossover and the Unitary Fermi Gas*, Lecture Notes in Physics Vol. 836 (Springer Science & Business Media, 2011).
[17] M. Randeria and E. Taylor, Annu. Rev. Condens. Matter Phys. **5**, 209 (2014).
[18] G. C. Strinati, P. Pieri, G. Röpke, P. Schuck, and M. Urban, Phys. Rep. **738**, 1 (2018).
[19] Y. Ohashi, H. Tajima, and P. van Wyk, Prog. Part. Nucl. Phys. **111**, 103739 (2020).
[20] C. A. Regal, M. Greiner, and D. S. Jin, Phys. Rev. Lett. **92**, 040403 (2004).
[21] M. W. Zwierlein, C. A. Stan, C. H. Schunck, S. M. F. Raupach, A. J. Kerman, and W. Ketterle, Phys. Rev. Lett. **92**, 120403 (2004).
[22] M. Bartenstein, A. Altmeyer, S. Riedl, S. Jochim, C. Chin, J. H. Denschlag, and R. Grimm, Phys. Rev. Lett. **92**, 203201 (2004).
[23] W. Ketterle and M. W. Zwierlein, Riv. Nuovo Cim. **31**, 247 (2008).
[24] K. O'Hara, New J. Phys. **13**, 065011 (2011).
[25] M. Horikoshi and M. Kuwata-Gonokami, Int. J. Mod. Phys. E **28**, 1930001 (2019).
[26] I. Bloch, J. Dalibard, and W. Zwerger, Rev. Mod. Phys. **80**, 885 (2008).
[27] J. E. Drut, J. R. McKenney, W. S. Daza, C. L. Lin, and C. R. Ordóñez, Phys. Rev. Lett. **120**, 243002 (2018).
[28] J. R. McKenney, A. Jose, and J. E. Drut, Phys. Rev. A **102**, 023313 (2020).
[29] R. Rajaraman and H. A. Bethe, Rev. Mod. Phys. **39**, 745 (1967).
[30] H.-W. Hammer, A. Nogga, and A. Schwenk, Rev. Mod. Phys. **85**, 197 (2013).
[31] N. Harshman and A. Knapp, Ann. Phys. (NY) **412**, 168003 (2020).
[32] N. L. Harshman and A. C. Knapp, Phys. Rev. A **105**, 052214 (2022).
[33] S. Ohya, Prog. Theor. Exp. Phys. **2024**, 013A01 (2024).
[34] S. Baiguera, Eur. Phys. J. C **84**, 268 (2024).
[35] W. S. Daza, J. E. Drut, C. L. Lin, and C. R. Ordóñez, Mod. Phys. Lett. A **34**, 1950291 (2019).
[36] Y. Fujimoto, K. Fukushima, L. D. McLerran, and M. Praszałowicz, Phys. Rev. Lett. **129**, 252702 (2022).
[37] S. Tan, Ann. Phys. (NY) **323**, 2952 (2008).
[38] S. Tan, Ann. Phys. (NY) **323**, 2971 (2008).
[39] S. Tan, Ann. Phys. (NY) **323**, 2987 (2008).
[40] E. Braaten, D. Kang, and L. Platter, Phys. Rev. Lett. **106**, 153005 (2011).
[41] F. Werner and Y. Castin, Phys. Rev. A **86**, 053633 (2012).
[42] M. Holten, L. Bayha, A. C. Klein, P. A. Murthy, P. M. Preiss, and S. Jochim, Phys. Rev. Lett. **121**, 120401 (2018).
[43] P. A. Murthy, N. Defenu, L. Bayha, M. Holten, P. M. Preiss, T. Enss, and S. Jochim, Science **365**, 268 (2019).
[44] J. Maki and C. R. Ordóñez, Phys. Rev. A **100**, 063604 (2019).
[45] H. Tajima, S. Tsutsui, T. M. Doi, and K. Iida, Phys. Rev. A **104**, 053328 (2021).
[46] H. Tajima, S. Tsutsui, T. M. Doi, and K. Iida, Phys. Rev. Res. **4**, L012021 (2022).
[47] L. McLerran and S. Reddy, Phys. Rev. Lett. **122**, 122701 (2019).
[48] H. Tajima, S. Tsutsui, T. M. Doi, and K. Iida, Symmetry **15**, 333 (2023).
[49] M. Klawunn and A. Recati, Phys. Rev. A **84**, 033607 (2011).
[50] M. Klawunn, Phys. Lett. A **380**, 2650 (2016).
[51] H. Sakakibara, H. Tajima, and H. Liang, Phys. Rev. A **107**, 053313 (2023).
[52] G. Bertaina and S. Giorgini, Phys. Rev. Lett. **106**, 110403 (2011).
[53] V. Makhalov, K. Martiyanov, and A. Turlapov, Phys. Rev. Lett. **112**, 045301 (2014).
[54] W. Ong, C. Cheng, I. Arakelyan, and J. E. Thomas, Phys. Rev. Lett. **114**, 110403 (2015).
[55] J. B. McGuire, J. Math. Phys. **7**, 123 (1966).
[56] M. Koschorreck, D. Pertot, E. Vogt, B. Fröhlich, M. Feld, and M. Köhl, Nature (London) **485**, 619 (2012).
[57] C. R. Hagen, Phys. Rev. D: Part. Fields **5**, 377 (1972).
[58] P. Ring and P. Schuck, *The Nuclear Many-Body Problem* (Springer Science & Business Media, Heidelberg, 2004).
[59] P. Niemann and H.-W. Hammer, Phys. Rev. A **86**, 013628 (2012).
[60] T. Kirk and M. M. Parish, Phys. Rev. A **96**, 053614 (2017).
[61] S. Akagami, H. Tajima, and K. Iida, Phys. Rev. A **104**, L041302 (2021).
[62] Y. Guo and H. Tajima, Phys. Rev. B **107**, 024511 (2023).
[63] S. Pilati and S. Giorgini, Phys. Rev. Lett. **100**, 030401 (2008).
[64] J. R. McKenney and J. E. Drut, Phys. Rev. A **99**, 013615 (2019).
[65] S. Zöllner, G. M. Bruun, and C. J. Pethick, Phys. Rev. A **83**, 021603(R) (2011).